

Gas Hydrates Inhibition via Combined Biomolecules and Synergistic Materials at Wide Process Conditions

Tausif Altamash¹ ϕ , M. Fahed Qureshi¹ ϕ , Santiago Aparicio^{2*}, Morteza Aminnaji³,
Bahman Tohidi³ and Mert Atilhan^{4*}

ϕ *Equal Contribution*

*Corresponding authors: sapar@ubu.es and mert.atilhan@qatar.tamu.edu

¹*Department of Chemical Engineering, Qatar University*

²*Department of Chemistry, University of Burgos, Spain*

³*Institute of Petroleum Engineering, Heriot Watt-University, United Kingdom*

⁴*Department of Chemical Engineering, Texas A&M University at Qatar*

ABSTRACT.

The motive of this research to present a systematic study in context of implementation of gas hydrate inhibitors that are obtained via naturally occurring amino acids (L-Alanine, Glycine, L-Histidine, L-Phenylalanine and L-Asparagine). These materials are tested for methane (CH₄) hydrate inhibition purposes from both thermodynamically and kinetically perspectives at wide process conditions. In this presented work, all studied amino acids have been tested at both 1 wt % as low dosage inhibitors as well as at higher concentrations up to 5 wt %. Furthermore, Polyethylene-oxide (PEO) and Vinyl Caprolactum (VCap) were used at 1 wt % in studied aqueous solutions as synergetic compounds to enhance the inhibition performance for CH₄ hydrate inhibition. Gas hydrate experiments were carried out by using rocking cell apparatus, from which pressure, temperature equilibrium data were obtained at recorded time and these data were translated into inhibitor performance evaluation from both thermodynamics and kinetic inhibition perspectives. This study includes the discussions of the effect of solubility limitation of studied amino acids, the effect of inhibitor concentration effect on the thermodynamic shift of the hydrate equilibrium curve, the role of side chain in amino acids in kinetic hydrate inhibition, the hydrophobic interactions of alkyl chain in water for synergistic point of

view. The results showed that the suitability of amino acids combined with synergistic materials for high kinetic inhibition performance, which provided an additional time shift up to 35 hours in hydrate formation at moderate process conditions up to 55 bars, specifically when L-Alanine was used.

Keywords: Gas hydrates; flow assurance; kinetic inhibitors; thermodynamic inhibitors; amino acids; synergetic compounds

1. INTRODUCTION

Natural gas exists in abundant quantities and being replaced coal for power generation in both industrial and residential applications due to its clean nature. Moreover, chemical process industries utilize natural gas as a starting material to produce syngas in various processes such as gas to liquid (GTL) and ethylene processes, where natural gas is the source of hydrogen gas.[1] The consumption of natural gas has been increased dramatically in the past couple of decades.[2] Typical natural gas production starts by drilling either at the seafloor or at onshore reservoirs and once the gas reservoir is tapped the gas is transported through the pipelines to a larger distribution pipe networks or direct to the gas processing facilities. During the course of gas transmission through the pipelines, there is a risk of gas hydrate cluster formation inside the pipeline and at other process equipment at low temperature and high pressure conditions,[3, 4] which leads to blockage in the pipelines and hinders the transportation of the flow the gas causing substantial economic losses and even catastrophic pipeline failures that might result in complete operation shutdowns.

Gas hydrates are crystalline and ice-like structures, which are formed by the coexistence of water molecules and gas hydrate former molecules (e.g. methane, ethane etc...). The favorable process conditions for the gas hydrate cages to occur is low temperatures and high pressures, which leads the formation of a network of hydrogen bonds (HO--H) in which gas hydrate former molecules are trapped and encapsulated within three-dimensional frameworks. The X-ray determination[5, 6] reveals that gas hydrate clusters mainly found in three types of molecular arrangements, cubic structure I (sI), cubic structure II (sII) and hexagonal structure H (sH), and the hydrate cage type depends upon the shape and/or size of the host gas or hydrate former gas molecule. For instance, CH₄, CO₂ and C₂H₆ leads to sI type hydrates, whereas C₃H₈ and iso-C₄H₁₀ molecules leads to sII type hydrate cage structure[7]. In order to prevent hydrate formation inside the gas transmission pipelines and provide flow assurance, gas hydrate inhibitors have been injected into the pipelines. Hydrate inhibitors are typically charged or polar compounds such as electrolytes, alcohols and glycols, which are classified as thermodynamic hydrate inhibitors. Amongst those typical inhibitors, methanol and mono-ethylene glycol have been proven to be the most effective ones.[8] On the other hand, unlike thermodynamic

inhibitors, kinetic hydrate inhibitors (typically water-soluble polymers) do not show significant shifting effect on the pressure (P) and temperature (T) hydrate equilibrium curve towards the hydrate safe region. Nevertheless, they show the effect of time delay for the growth of hydrate crystals in which the hydrate inhibition is applied[9]. Some surfactants act as anti-agglomerates via forming aggregates leaving the hydrate particles as tiny particles and hinder their growth within the pipeline.[10] Such conventional inhibitors injected in large quantities during pipeline operations and the risk of toxic materials spillage to the surrounding aquatic system is high and dangers the habitat. Therefore, in order to prevent environmental hazards due to the excessive usage of high toxic nature chemicals in the pipelines, environmentally benign chemicals have been searched by both academia and industry in order to replace the toxic ones. It is also aimed to reduce the cost of the intervention in the case pipeline is under the hydrate formation risk by reducing the amount of the used chemicals as well as reduce or eliminate the cost of the recovery of the injected chemicals to the pipeline. Search for alternative thermodynamic and kinetic inhibitors such as urea,[11] chitosan,[12] proteins[9] and synthetic bio-molecules have been used as gas hydrate inhibitors in recent years as being alternative inhibitors in order to tackle above-mentioned challenges.[13-16]

Amino acids are model compounds of proteins and they are also found in genetic coding as the fundamental building blocks known life forms in our planet.[17] Among 500 known amino acids, only 20 of those appear in genetic coding and these synthesized amino acids are frequently used in animal feed additives, flavor enhancers, cosmetics ingredients and medicinal products.[18] Moreover, amino acids were also used as corrosion inhibitors and due to their negligible negative impact on aquatic systems.[19-21] Chemically, amino acids have zwitterion, which contains carboxylic (-COOH) and ammonium (-NH₂) groups attached to the center C atom, and yet some amino acids also contain an additional carboxylic acid, amide, phenyl, imidazolium and alkyl chains. These additional groups determine the nature of amino acid such as acidity/basicity or hydrophilicity/hydrophobicity. Amino acid molecules in water accessing zwitterion-ion, zwitterion-water-dipoles, ions-water-dipole interactions with water molecule as well as other ions present in aqueous systems.[17, 22-24] The electrostatic force of attraction capability of an amino acid can have an effect on liquid water structure and might lead to a prevention of

hydrogen bonding during the hydrate cage formation around the hydrate former and guest gas molecule. Raman spectroscopy technique has been proven that, hydrophilic or hydrophobic moieties disrupt or strengthening the water structures.[25] Sloan and Koh[26] also postulated that hydrogen bonding and electrostatic interactions lower the activity coefficient of water, and thus thermodynamic inhibition takes place.

Natural gas consists of complex multi-component gas mixtures and as documented elsewhere[27-29] methane (CH₄) is the major constituent of natural gas reservoirs. In this work, rather than dealing with complex multi component gas mixtures, which can lead to different hydrate cage formations, CH₄ has been studied as a representative model for natural gas to study gas hydrate inhibition performance of amino acids. Having said that, in the case of actual pipeline conditions gas hydrates are formed in both sI and sII type; in this proof of concept experimental work, methane is used and only sI type of hydrate formation is observed. A number of researchers presented their reports using amino acids as inhibitor for kinetic, thermodynamic studies for CO₂, CH₄ and tetrahydrofuran gas hydrates.[13, 14, 16, 30] This study provides a detailed study of thermodynamic and kinetic methane hydrate inhibition performance together by using Glycine, L-Alanine, L-Histidine, L-Phenylalanine and L- Asparagine amino acids as inhibitors at both low and high doses at various process conditions that includes pressures between 40 to 120 bars. Moreover, a combined synergized behavior of amino acids was also studied for enhanced kinetic inhibition purposes by adding 1 wt% of water soluble polymer/monomer (polyethylene oxide/vinyl caprolactum) into the L-Alanine Glycine and L-Histidine solutions at above-mentioned pressure ranges.

2. EXPERIMENTAL SECTION

2.1. Materials

CH₄ gas with the purity of 99.9% was purchased from Buzware Scientific and Technical Gases, Doha (Qatar). Amino acids and synergents were purchased from Sigma-Aldrich and the details of the purities, structures and molar masses of these samples are provided in Table 1. All the aqueous samples were prepared in Millipore quality distilled water (Milli-Q, Millipore, resistivity 18.2 MΩ cm) by weighing on an Mettler Toledo XS105 electronic balance with a precision of ± 0.00001 g.

Table 1:

2.2. Apparatus and Methods

Rocking cell is an assembly of five cells parallel working at a same skid (RC-5) has been purchased from PSL SystemtechniK GmbH, Germany. RC-5 assembly is capable of operating at pressures up to 200 bar (2900 psi) and has temperature rating of $-10\text{ }^{\circ}\text{C}$ to $60\text{ }^{\circ}\text{C}$. Each high-pressure rocking cell has a volume of 40.13 cm^3 and it encapsulates a stainless steel ball with the diameter of 17 mm, which moves back and forth and provides agitation within the cell. There are total 5 rocking cells installed on a metal plate and the assembly is submerged in a cooling-heating bath for thermostating purposes. The mixing inside the cells is carried out by rocking with a pre-defined frequency of 10 rocks/min and with the rocking angle of 30° . [31] Cells were pressurized directly with cylinder pressure of gas in the range of 30 to 120 bars at different desired pressure intervals and pressures within the cells were fine-tuned with high pressure hand pump. Operational method of RC-5 during the course of experiments, programmed protocol for temperature cycle and sample loading have been described in detail elsewhere. [31-38] Cooling-heating bath was connected to an external cooling circulator, Huber Ministat 125w, and is capable of operating temperatures between -25 and $150\text{ }^{\circ}\text{C}$. Apparatus temperature sensors have an accuracy of $\pm 0.25\text{ }^{\circ}\text{C}$ and pressure sensors of the apparatus have an accuracy of 0.1% of pressure full scale (standard uncertainties, u , are $u(P) = 0.02\text{ bar}$, $u(T) = 0.25\text{ }^{\circ}\text{C}$).

Prior to each experiment, rocking cells are carefully flushed and purged with the sample that will be used during the new experiments. Rocking cells are pressurized up to the target pressures for each rocking cell. Then temperature/pressure stabilization is obtained within each rocking cell, only after that data acquisition is started to execute the experimental protocol. The experimental protocol follows: (i) initialization phase of the rocking cells experiment was started to stabilize the cell temperature around $20\text{ }^{\circ}\text{C}$ initial temperature for over a two hours. During this period any pressure losses and gas leaks are also observed. (ii) The experimental runs were then started by cooling the fluid inside vessel (in which the rocking cells are submerged) with the cooling rate of $(1.8\text{ }^{\circ}\text{C/hr})$ from $20\text{ }^{\circ}\text{C}$ to $2\text{ }^{\circ}\text{C}$ with an agitation of 10 rocks/min, then the system was left for 24 hours at $2\text{ }^{\circ}\text{C}$ to form hydrates. Targeted sub-cooling temperature is around 6 to $8\text{ }^{\circ}\text{C}$, which depends on the hydrate former as well as the initial starting pressure. Once the hydrate is formed within the rocking cell

(observed via pressure drop), the rocking ball stop rolling and plugs the cell. (c) Heating process was started back to the initial temperature with very slow rate (0.18 °C/hr) for complete hydrate melting, after the hydrate is obtained within the cell. A controlled step-wise heating was used for hydrate dissociation and 12 hours of intermission has been given at every 12 hours. This makes an approximate heating rate of 1.44 °C per day.

A typical experimental procedure on how to obtain hydrate Pressure-Temperature loop in an isochoric pressure search method using rocking cell assembly is given in a previous work.[39] The hydrate equilibrium point is obtained after solving the intersection point of hydrate dissociation trace and cooling trace linear fittings.[39] Collected hydrate equilibrium pressure-temperature data is reported as the typical data set not as average values in this manuscript.

Density of aqueous solutions was measured at different temperatures using Anton Paar DMA 4500M apparatus, which operates by using oscillating U-tube sensor principle and only 1 mL of sample required to get density results. The standard uncertainties, u , for density measurements are $u(P) = 0.05$ bar, $u(T) = 0.05$ K, combined standard uncertainty in density is $u(\rho) = 0.00005$ g m⁻³. [40]

3. METHODOLOGY

The study of phase equilibrium of gas hydrate formation and dissociation has been done to show the thermodynamics effect and determine induction time in order to solve kinetics of the inhibitor effect by plotting temperature-pressure (P-T) and time-pressure (t-P) results respectively.[41, 42] Through the processing of P-T or t-P data curves, the effect of additives used as inhibitors can be identified and their effect with respect to alternating pressure conditions can also be identified. In order to meet certain environmental regulations that are explained in the introduction section of this manuscript, naturally occurring bio-molecules such as amino acids as neat alternative inhibitors were introduced to the hydrate inhibition experiments in this work. The variation in molecular structure of the amino acids directly affects hydrogen bonding and electrostatic interactions in aqueous environment in which they are utilized. Hydrophobicity and hydrophilicity of amino acid related to charged side, or alkyl chain or group that alters the interaction with water molecule causes aqueous solubility. In water bulk, carboxylic (–COOH) and amine (–NH₂)

group of amino acid turn into zwitterion ($-\text{COO}^-$ and NH_3^+), [23] where water molecule binds with zwitterion from their opposite pole sites and form a strong hydration shell around, as a result disruption of hydrogen bond occurs. On the basis of unique molecular structures of each amino acid (side chain), five different amino acids have been targeted as inhibitor for CH_4 hydrate at different pressures, and programmed via high-low-high temperature cycles at identical water cuts in each high pressure cell. CH_4 hydrate inhibition studied firstly by adding amino acids as 1 wt% as low dosage inhibitors. Later, this concentration has been increased to higher doses of either 4 wt% or 5 wt% based on the solubility values at room temperature for each amino acid.

On the other hand, few studies have been described the action of a PEO polymer in water, which acts as a synergistic compound. **PEO is not hazardous and is not dangerous in the form in which it is placed on commercial market and PEO; moreover in terms of ecological toxicity, PEO is not considered to be toxic in the aquatic environment.** Hammouda and Kline[43] described the force interaction driving of PEO with water using small-angle neutron scattering as: (i) hydrogen bonding between oxygen atoms with H_2O ; (ii) hydrophobic interaction between polymer-polymer ($\text{CH}_2\text{-CH}_2$) and tend to repel water molecule. Boucher and Hines[44, 45] provided breakthrough information that PEO-water solution fully soluble at moderate temperature but solution becoming turbid on higher temperature. Reven et al.[46] observed best chain mobility of PEO amongst water-saturated hydrogen-bonded polymer complexes. Thus reasonably good solubility of PEO in water at lower temperature and their hydrophobic/hydrophilic action in water facilitates to work with inhibitor to achieve new scale of gas hydrate inhibition. Vcap has been used as copolymer to prepare commercially available Luvicap 55W polymer for natural gas hydrate inhibition purpose.[47] In this work, VCap as monomer was tested to evaluate its synergistic property, despite the oxygen atom of VCap disturb the hydrogen bonding via making hydrogen bonding by own and hydrophobic caprolactum ring interact with hydrate surface with van der van der Waals interactions.[47-49]

4. RESULTS AND DISCUSSIONS

4.1 Pure Methane Hydrate Experiments

The data reproducibility and calibration of RC-5 instrument were previously done by using both pure and multi-component gas mixtures and the data for pure CH₄ gas-hydrate equilibrium calibration experimental data and its comparison with previously published data is provided in Table 2. [31, 32, 50, 51]

Table 2

For the consistency purposes, all RC-5 cells have been calibrated and validated prior to their use for this study. For calibration purposes, experiments have been conducted with high-low-high temperature cycle to form and dissociate CH₄ hydrates in presence of de-ionized water within the cells at five different initial starting pressures that ranges from approximately 40 to 120 bars. These calibration results were plotted with existing published data[50, 51] in Figure S1 (available in supporting information).

4.2 Amino Acids as Thermodynamic Inhibitors

Aqueous solutions of all amino acids viz., Glycine, L-Alanine, L-Phenylalanine, L-Histidine and L-Asparagine have been prepared at identical water cuts filled in rocking cells, and cells were pressurized with CH₄ at different initial starting cell pressures (e.g. 120, 100, 80, 60 and 40 bars). In low dosage hydrate inhibitor test experiments, 1 wt% of each amino acid has been used for CH₄ hydrate inhibition, and for higher dosage experiments, 5 wt% of Glycine, and L-Alanine and maximum solubility of 4 wt % of L-Histidine were used for the investigation of the dosage effect (concentration effect) on hydrate equilibrium.

Figure 1:

In the presence of low and high dosage of amino acids, hydrate dissociation temperature values are summarized against pressures in Table 3. Figure 1 and Figure 2 show graphical representation of CH₄ hydrate equilibrium curves with the absence and presence of amino acids and allow comparison of the both conditions. Figure 1 demonstrates hydrate inhibition performance at 1 wt% amino acids, where almost null inhibition was observed, despite the drop in the hydrate dissociation points on CH₄ hydrate curve, which clarify that low dosage amino acids cannot be considered as an effective thermodynamic inhibitors at this low concentrations.

Figure 2:

Table 3:

Consequently, increased amount of inhibitor dosages has been tested to evaluate inhibition action and those experimental temperature-pressure data points were given in Figure 2. It was observed that the dissociation points of $\text{CH}_4 + \text{H}_2\text{O} + \text{amino acid}$ system does not show enhancement in hydrate inhibition performance at lower concentrations. However, a close perusal of Figure 2 reveals that, 5 wt% Glycine and L-Alanine have shown improvement in the inhibition effect significantly, nevertheless L-Histidine found to be inactive even at 4 wt% concentration.

5 wt% Glycine and L-Alanine dissociation points were shifted toward low temperature zone of hydrate inhibition. L-Glycine and L-Alanine at pressures lower than 40 bar, temperature was shifted maximum by $0.8\text{ }^\circ\text{C}$ from the original $\text{CH}_4 + \text{H}_2\text{O}$ hydrate pressure-temperature equilibrium calibration curve. This improved behavior of equilibrium shift at higher concentration of amino acids was expected thermodynamic inhibition phenomena. The density plot (Figure S2 of electronic supporting information) of amino acids at different concentration and with PEO or VCap shows that on increasing the amount of inhibitor means availability of inhibitor's molecules in per unit volume of H_2O increased, thus number of hydrogen bonds disruption increases and gas hydrate clustering process is inhibited. Indeed, the failure of thermodynamic inhibition with high dosage (4 wt. %) of L-Histidine occurred due to solubility issues. The solubility index of amino acids reveals that maximum solubility of L-Histidine is $4.19\text{ g}/100\text{ g}$ at $25\text{ }^\circ\text{C}$ [52]. 4 wt.% of L-Histidine was at the verge of solubility limit in aqueous solution at room temperature ($25\text{ }^\circ\text{C}$) and during the experimental operation temperature starts from $20\text{ }^\circ\text{C}$ to lower degree of temperature where precipitation takes place within the high pressure cells. With respect to the further explanation on structural ground of inhibition via amino acids; glycine is the simplest structure of all the amino acids due to presence of a hydrogen atom on side chain position, whereas one additional $-\text{CH}_3$ group present on side chain. The least side chain availability allows them to mix with water molecules completely, therefore methyl group of alanine does not have a remarkable effect. Hereupon, glycine and alanine shows similar thermodynamic inhibition performance in Figure 2. J-H. Sa and coworkers[16] also studied amino acids as CO_2 hydrate inhibitors at pressures less than 40 bar and at different mole

concentrations. Our thermodynamic inhibition results agreed in parallel with their statements; (i) higher the concentration of amino acids better the hydrate inhibition performance; (ii) amino acids with solubility limits for which the concentrations exceeded aqueous solubility limit leaves undissolved particles and leads to precipitation from the aqueous phase; and thus does not take part in the inhibition process and does not show remarkable difference in the hydrate pressure-temperature equilibrium curve obtained for saturated or supersaturated amino acid aqueous solutions; (iii) Glycine and L-Alanine have been identified as potential natural gas hydrate inhibitors for thermodynamic hydrate inhibition purposes.

Furthermore, in order to understand the molecular significance of amino acids moles have been calculated from 5 grams of L-Alanine and Glycine, and 4 grams L-Histidine, which is equal to 5 wt% and 4 wt% respectively and yield to molar amounts of 0.0561 moles of L-Alanine, 0.0666 moles of Glycine and 0.0258 moles of L-Histidine. Among the prepared solutions, the one that contains L-Histidine has the least amount of mole, which is due to the existence of an imidazole side chain in its structure. However, presence of low mole in water may not lead to form water-amino acid association significantly and thus it does not provide appreciable hydrate inhibition effect accordingly.

4.3 Amino Acids as Kinetic Inhibitors

Kinetics of CH₄ hydrate inhibition has been also investigated in this study via observing the change in time delay that takes place during the hydrate formation takes place in the experimental setup. Time delay is compared in the case of inhibitor presence and existence cases for benchmarking the effect of amino acids as kinetic inhibitors. Like thermodynamic inhibition experiments, kinetic inhibition experiments also carried out at different pressures that resembles the wide range of actual pipeline operation conditions. The dissociation points of all amino acids have been summarized in Table 4 and plotted in Figure 3 as time vs pressure.

Figure 3:

Figure 3 shows that every amino acid at 1 wt% has capability to change the time delay from solid line (CH₄+ H₂O) except L-Histidine. At lower pressures (P < 40 bar) L-Phenylalanine poses maximum delay among other inhibitors and time delay shift trend

observed as L-Phenylalanine > L-Asparagine \approx Glycine \approx L-Alanine > L-Histidine. L-Asparagine shows significant time delay in hydrate formation at 56 bar and 110 bar, whereas insignificant time delayed was observed at pressures 75 and 95 bar.

Table 4:

There were also some points observed at which no particular time delay trends can be obtained. An increased amount of amino acid does not contribute much to the time delay effect despite the use of the inhibitor at multiple times more dosages. Contrary, a close scrutiny reveals that L-Histidine at 4 wt% delay more nucleation time at 1 wt% at each pressure (Figure 4).

Figure 4:

Sa et al[15, 25] presented simulation and experimental results on the kinetic inhibition studies that uses various amino acids highlighting that Glycine and L-Alanine are the ones that provides appreciable kinetic inhibition performance. Moreover, they also reported that with the increasing of the concentration of the amino acids they did not encounter significant change in the nucleation. Roosta et.al[14] and Naeji[13] also reported that Glycine molecule actively participated in kinetic gas hydrate inhibition with CO₂ system at 30 bar and also with tetrahydrofuran at atmospheric pressure.

4.4 Synergistic Effect Experiments

In order to test the synergistic gas hydrate inhibition effect; vinylcaprolactum (VCap) and poly-ethylene-oxide (PEO) has been added into aqueous solution of 5 wt.% of Glycine, 5 wt.% of L-Alanine and 4 wt.% of L-Histidine amino acids as 1 wt% and synergistic effect experiments were carried out at four different pressures of CH₄ with previously explained temperature cooling-heating protocol. Similarly, experimental pressure, temperature and time data were collected and used in order to identify the hydrate dissociation point as well as the time delay for both thermodynamic and kinetics studies respectively. The dissociation points data for VCap + amino acids are summarized in Table 5 and they are plotted in Figure 5.

Figure 5:

According to the obtained data, VCap + Glycine and VCap + L-Alanine combinations did not provide significant effect on the shift of the hydrate equilibrium curve towards

inhibition or hydrate safe region and also they did not show capabilities to provide superior performance when they are compared with amino acids solely (without VCap) at same concentrations.

Figure 6:

In Figure 6, PEO + amino acids thermodynamic inhibition data is given. Figure 6 reveals weak thermodynamic inhibition performance. This result was expected since PEO has a more kinetic effect rather than thermodynamic effect, when it is combined with an inhibitor.[53]

Table 5:

The kinetic studies have also been investigated for amino acid + VCap and amino acid + PEO combinations in order to evaluate the time delay in hydrate formation and these results are given in Figure 7.

Figure 7:

VCap + amino acid combinations show a remarkable time delay at lower pressures (40 to 60 bar), however these results are not more than the time delay results that was obtained for the case that does not include VCap. Thus, VCap detected as an incapable as synergist neither for thermodynamic nor for the kinetic hydrate inhibition applications. Amino acid + PEO case at different pressures have been summarized in Table 6, and plotted in Figure 8.

Table 6:

Figure 8:

A steep trend was shown in the Figure 8 as the pressure increases, delay in hydrate formation reduces. From pressure range 80 to 105 bar insignificant time delay was observed comparatively to that of lower pressures. The most remarkable aspect of Figure 8 was observed for L-Alanine + PEO combination that resulted approximately 35 hr of time delay in hydrate formation at a pressure of 56 bars, which was noted as an extraordinarily high induction for this study and is equivalent to four folds of time delay than L-Alanine posed by itself. Although it has been postulated by Lee and Englezos[54] that PEO triggers the kinetic inhibition effect when it is combined with a kinetic inhibitor compounds, categorically our case study revealed that at around 55 bars all three amino acids that are combined with 1 wt% of PEO have ability to alter the time delay in gas

hydrate formation exponentially. The trend of effectiveness of amino acids + PEO system as kinetic inhibitor for CH₄ hydrates were observed as; L-Alanine > Glycine > L-Histidine. At pressure higher than 55 bar, L-Histidine shows better performance than L-Glycine and L-Alanine but a systematic trend was not observed due to the difference in experimental pressures (e.g. 62, 65 and 72 bars respectively).

Figure 9:

Figure 9 shows the composition of PEO combination with L-Histidine at 4% and with Glycine at 5%, which represent imidazole side chain help in kinetic inhibition in presence synergents rather than to diminishing. Interestingly, L-Alanine, Glycine and L-Histidine given same time delay of 12 hr at pressures 86, 81, and 83 bar respectively. Synergism or synergistic effect of amino acids + PEO mixture can be described in terms of interactions with water molecules. Water-soluble PEO contains hydrophilic oxygen atoms in the center and polymerized hydrophobic ethylene chain attached with oxygen atom. At one side hydrophobic polymeric chain pushes the water molecule away from CH₄ by operating van der Waals hydrophobic interactions and provides shield over the potential hydrate cage. Whereas at another side, hydrophilic oxygen atoms form hydrogen bonds through electrostatic force of attraction (CH₂O---HOH---OCH₂) causing forward the time of nucleation. In the presence of water, amino acid act as hydrate inhibitor due to zwitterions (NH₃⁺/CHOO⁻) solvation, hence disruptions occur within water. The individual effect of PEO and amino acids turn into synergistic effect as add them collectively (PEO + amino acid) in aqueous environment. In other words, by mixing PEO with amino acids, such enhancement of kinetic inhibition of ILs upon addition of polymeric synergents indicates that they may have nucleation hydrate inhibition effect rather than hydrate crystal growth inhibition effect. And similar conclusion can be made for the PVCap as its molecules disrupt the organization of water-gas molecules, increasing the barrier to nucleation with less impact then PEO can provide. The increased value of time delay in hydrate growth of L-Alanine in comparison with Glycine at similar pressure, temperature and concentration indicates that the presence of -CH₃ at L-alanine side chain enhance the hydrophobic interaction (H₃C—CH₂) with PEO. The cause of synergistic effect in the presence of duo suggested that as soon as PEO enters into water bulk prevent the approach of water molecule towards CH₄ through hydrophobic interaction and unaffected water molecule

disrupt by amino acids at water-CH₄ interface. In their isochoric based gas hydrate equilibrium experiments, Kang et al.[48] reported twice induction time of CH₄ hydrate growth with of PVCap + [HEMP][BF₄] ionic liquids than that of ionic liquid alone and provide an explanation of similar mechanism of synergistic effect of combination.

Figure 10:

Figure 10 has been plotted to represent the comparison of induction time between amino acids + PEO mixture of this study and recently published results of polyVCap + ionic liquid mixture for CH₄ and natural gas hydrate inhibition, which were obtained through similar isochoric based gas hydrate equilibrium experiments.[48, 55] As a result of examining the synergistic effect, hydrophobic chain of a polymer signified as the strongest part to synergize the inhibitor performance by repelling water molecule away from gas as a result that causes observed time delays.

Moreover, it is important to mention that 5 wt% VCap and ionic liquids composition given a significant thermodynamic synergistic inhibition effect in our previous work.[31] Higher amount of inhibitors always support the thermodynamic inhibition performance despite the oxygen atom at carbonyl group of VCap attributed to hydrogen bonding with water molecule.[49] As far as kinetic of synergistic effect for VCap, it has been found to be incapable to do so simply because of the absence of the long polymeric chain. 1 wt% of VCap was further investigated with the presence of 5 wt% L-Alanine for a previously studied quaternary gas mixture (e.g. methane, ethane, nitrogen and carbon dioxide)[31] at different pressures to compare with CH₄ hydrate inhibition. Figure S3 and Figure S4 illustrate similar trend of inhibition behavior for both thermodynamic and kinetic inhibition effects.

5. CONCLUSIONS

In this work, we showed the capability of gas hydrate inhibitor performances of amino acids from both thermodynamic and kinetic inhibition perspectives. Low concentrations of amino acids showed poor thermodynamic and kinetic inhibition performances. At higher concentrations, some amino acids showed slight improvement in hydrate inhibition. However, when amino acids were coupled with synergistic effect additives, they have shown extraordinarily superb kinetic inhibition effect, which was explained by the

complicated interactions of the prepared compound complex with surrounding water molecules. L-Alanine in combination with PEO system has shown remarkably high kinetic inhibition performance with approximately 35 hr of time delay in hydrate formation at pressure of 56 bar in this study; which is indeed 4 folds of time induction effect when L-Alanine itself is considered. As a summary, amino acids can be considered as environmentally friendly kinetic inhibitors when coupled with select synergistic additives.

Acknowledgement

This work was made possible by NPRP grant # 6-330-2-140 and GSRA # 2-1-0603-14012 from the Qatar National Research Fund (a member of Qatar Foundation). The statements made herein are solely the responsibility of the authors.

REFERENCES

- [1] S. Park, Y. Bang, S.J. Han, J. Yoo, J.H. Song, J.C. Song, J. Lee, I.K. Song, Hydrogen production by steam reforming of liquefied natural gas (LNG) over mesoporous nickel–iron–alumina catalyst, *International Journal of Hydrogen Energy*, 40 (2015) 5869-5877.
- [2] A.S. Brown, A.M.H. van der Veen, K. Arrhenius, M.L. Downey, D. Kühnemuth, J. Li, H. Ent, L.P. Culleton, Traceable Reference Gas Mixtures for Sulfur-Free Natural Gas Odorants, *Analytical Chemistry*, 86 (2014) 6695-6702.
- [3] B. Kvamme, T. Kuznetsova, J.M. Bauman, S. Sjöblom, A. Avinash Kulkarni, Hydrate Formation during Transport of Natural Gas Containing Water and Impurities, *Journal of Chemical & Engineering Data*, 61 (2016) 936-949.
- [4] Z.M. Aman, C.A. Koh, Interfacial phenomena in gas hydrate systems, *Chemical Society Reviews*, 45 (2016) 1678-1690.
- [5] J.S. Loveday, R.J. Nelmes, M. Guthrie, S.A. Belmonte, D.R. Allan, D.D. Klug, J.S. Tse, Y.P. Handa, Stable methane hydrate above 2[thinsp]GPa and the source of Titan's atmospheric methane, *Nature*, 410 (2001) 661-663.

- [6] C.A. Koh, Towards a fundamental understanding of natural gas hydrates, *Chemical Society Reviews*, 31 (2002) 157-167.
- [7] E.D. Sloan, Fundamental principles and applications of natural gas hydrates, *Nature*, 426 (2003) 353-363.
- [8] M.D. Jager, C.J. Peters, E.D. Sloan, Experimental determination of methane hydrate stability in methanol and electrolyte solutions, *Fluid Phase Equilibria*, 193 (2002) 17-28.
- [9] M.A. Kelland, History of the Development of Low Dosage Hydrate Inhibitors, *Energy & Fuels*, 20 (2006) 825-847.
- [10] A. Kumar, T. Sakpal, R. Kumar, Influence of Low-Dosage Hydrate Inhibitors on Methane Clathrate Hydrate Formation and Dissociation Kinetics, *Energy Technology*, 3 (2015) 717-725.
- [11] S. Muromachi, T. Abe, T. Maekawa, Y. Yamamoto, Phase equilibrium for clathrate hydrate formed in methane + water + urea system, *Fluid Phase Equilibria*, 398 (2015) 1-4.
- [12] Y. Xu, M. Yang, X. Yang, Chitosan as green kinetic inhibitors for gas hydrate formation, *Journal of Natural Gas Chemistry*, 19 (2010) 431-435.
- [13] P. Naeiji, A. Arjomandi, F. Varaminian, Amino acids as kinetic inhibitors for tetrahydrofuran hydrate formation: Experimental study and kinetic modeling, *Journal of Natural Gas Science and Engineering*, 21 (2014) 64-70.
- [14] H. Roosta, A. Dashti, S.H. Mazloumi, F. Varaminian, Inhibition properties of new amino acids for prevention of hydrate formation in carbon dioxide–water system: Experimental and modeling investigations, *Journal of Molecular Liquids*, 215 (2016) 656-663.
- [15] M. Shatat, M. Worall, S. Riffat, Opportunities for solar water desalination worldwide: Review, *Sustainable Cities and Society*, 9 (2013) 67-80.
- [16] J.-H. Sa, B.R. Lee, D.-H. Park, K. Han, H.D. Chun, K.-H. Lee, Amino Acids as Natural Inhibitors for Hydrate Formation in CO₂ Sequestration, *Environmental Science & Technology*, 45 (2011) 5885-5891.
- [17] Riyazuddeen, T. Altamash, A. Coronas, Interactions in l-histidine/l-glutamic acid/l-tryptophan/glycylglycine + 2 mol L⁻¹ aqueous KCl/KNO₃ systems at different temperatures: An isothermal compressibility study, *Thermochimica Acta*, 543 (2012) 313-317.

- [18] K. Ivanov, A. Stoimenova, D. Obreshkova, L. Saso, *Biotechnology in the Production of Pharmaceutical Industry Ingredients: Amino Acids, Biotechnology & Biotechnological Equipment*, 27 (2013) 3620-3626.
- [19] K. Barouni, L. Bazzi, R. Salghi, M. Mihit, B. Hammouti, A. Albourine, S. El Issami, Some amino acids as corrosion inhibitors for copper in nitric acid solution, *Materials Letters*, 62 (2008) 3325-3327.
- [20] V. Hluchan, B.L. Wheeler, N. Hackerman, Amino acids as corrosion inhibitors in hydrochloric acid solutions, *Materials and Corrosion*, 39 (1988) 512-517.
- [21] M. Dehdab, M. Shahraki, S.M. Habibi-Khorassani, Theoretical study of inhibition efficiencies of some amino acids on corrosion of carbon steel in acidic media: green corrosion inhibitors, *Amino Acids*, 48 (2016) 291-306.
- [22] Riyazuddeen, T. Altamash, Viscosities of 1-Histidine/l-Glutamic Acid/l-Tryptophan/Glycylglycine + 2 M Aqueous KCl/KNO₃ Solutions at T = (298.15 to 323.15) K, *International Journal of Thermophysics*, 32 (2011) 1148-1162.
- [23] Riyazuddeen, T. Altamash, Study of interactions of 1-histidine/l-glutamic acid/l-tryptophan/glycylglycine with KCl/KNO₃ at different temperatures: 298.15, 303.15, 308.15, 313.15, 318.15, 323.15 K, *Thermochimica Acta*, 501 (2010) 72-77.
- [24] Riyazuddeen, T. Altamash, Ultrasonic Velocities and Densities of 1-Histidine or l-Glutamic Acid or l-Tryptophan or Glycylglycine + 2 mol·L⁻¹ Aqueous KCl or KNO₃ Solutions from (298.15 to 323.15) K, *Journal of Chemical & Engineering Data*, 54 (2009) 3133-3139.
- [25] J.-H. Sa, G.-H. Kwak, K. Han, D. Ahn, K.-H. Lee, Gas hydrate inhibition by perturbation of liquid water structure, *Scientific Reports*, 5 (2015) 11526.
- [26] Hydrate Formation and Dissociation Processes, in: *Clathrate Hydrates of Natural Gases*, Third Edition, CRC Press, 2007, pp. 113-187.
- [27] IPCC reports, Fifth Assessment Report; Intergovernmental Panel on Climate Change, <https://http://www.ipcc.ch/>.
- [28] D. Zavala-Araiza, D. Lyon, R.A. Alvarez, V. Palacios, R. Harriss, X. Lan, R. Talbot, S.P. Hamburg, Toward a Functional Definition of Methane Super-Emitters: Application to Natural Gas Production Sites, *Environmental Science & Technology*, 49 (2015) 8167-8174.

- [29] M. Tariq, M. Atilhan, M. Khraisheh, E. Othman, M. Castier, G. García, S. Aparicio, B. Tohidi, Experimental and DFT Approach on the Determination of Natural Gas Hydrate Equilibrium with the Use of Excess N₂ and Choline Chloride Ionic Liquid as an Inhibitor, *Energy & Fuels*, 30 (2016) 2821-2832.
- [30] J.-H. Sa, G.-H. Kwak, K. Han, D. Ahn, S.J. Cho, J.D. Lee, K.-H. Lee, Inhibition of methane and natural gas hydrate formation by altering the structure of water with amino acids, *Scientific Reports*, 6 (2016) 31582.
- [31] M.F. Qureshi, M. Atilhan, T. Altamash, M. Tariq, M. Khraisheh, S. Aparicio, B. Tohidi, Gas Hydrate Prevention and Flow Assurance by using Mixtures of Ionic Liquids and Synergent Compounds: Combined Kinetics and Thermodynamic Approach, *Energy & Fuels*, (2016).
- [32] E.C. Mohammad Tariq, Jillian Thompson, Majeda Khraisheh, Mert Atilhan, David Rooney, Doubly dual nature of ammonium-based ionic liquids for methane hydrates probed by rocking-rig assembly, *RSC Advances*, 6 (2016) 23827-23836.
- [33] B. Tohidi, R.W. Burgass, A. Danesh, K.K. ØStergaard, A.C. Todd, Improving the Accuracy of Gas Hydrate Dissociation Point Measurements, *Annals of the New York Academy of Sciences*, 912 (2000) 924-931.
- [34] M.A. Clarke, P.R. Bishnoi, Determination of the intrinsic kinetics of CO gas hydrate formation using in situ particle size analysis, *Chemical Engineering Science*, 60 (2005) 695-709.
- [35] B. ZareNezhad, F. Varaminian, A generalized macroscopic kinetic model for description of gas hydrate formation processes in isothermal–isochoric systems, *Energy Conversion and Management*, 57 (2012) 125-130.
- [36] R. Ohmura, S. Takeya, T. Uchida, T. Ebinuma, Clathrate Hydrate Formed with Methane and 2-Propanol: Confirmation of Structure II Hydrate Formation, *Industrial & Engineering Chemistry Research*, 43 (2004) 4964-4966.
- [37] M. Mohammad-Taheri, A. Zarringhalam Moghaddam, K. Nazari, N. Gholipour Zanjani, The role of thermal path on the accuracy of gas hydrate phase equilibrium data using isochoric method, *Fluid Phase Equilibria*, 338 (2013) 257-264.

- [38] A.P. Semenov, V.I. Medvedev, P.A. Gushchin, V.S. Yakushev, Effect of heating rate on the accuracy of measuring equilibrium conditions for methane and argon hydrates, *Chemical Engineering Science*, 137 (2015) 161-169.
- [39] N.A. Mohamed, M. Tariq, M. Atilhan, M. Khraisheh, D. Rooney, G. Garcia, S. Aparicio, Investigation of the performance of biocompatible gas hydrate inhibitors via combined experimental and DFT methods, *The Journal of Chemical Thermodynamics*, 111 (2017) 7-19.
- [40] R. Ullah, M. Atilhan, B. Anaya, M. Khraisheh, G. Garcia, A. ElKhattat, M. Tariq, S. Aparicio, A detailed study of cholinium chloride and levulinic acid deep eutectic solvent system for CO₂ capture via experimental and molecular simulation approaches, *Physical Chemistry Chemical Physics*, 17 (2015) 20941-20960.
- [41] M. Tariq, D. Rooney, E. Othman, S. Aparicio, M. Atilhan, M. Khraisheh, Gas Hydrate Inhibition: A Review of the Role of Ionic Liquids, *Industrial & Engineering Chemistry Research*, 53 (2014) 17855-17868.
- [42] M.F. Qureshi, M. Atilhan, T. Altamash, S. Aparicio, M. Aminnaji, B. Tohidi, High-pressure gas hydrate autoclave hydraulic experiments and scale-up modeling on the effect of stirring RPM effect, *Journal of Natural Gas Science and Engineering*, 38 (2017) 50-58.
- [43] B. Hammouda, D. Ho, S. Kline, SANS from Poly(ethylene oxide)/Water Systems, *Macromolecules*, 35 (2002) 8578-8585.
- [44] E.A. Boucher, P.M. Hines, Effects of inorganic salts on the properties of aqueous poly(ethylene oxide) solutions, *Journal of Polymer Science: Polymer Physics Edition*, 14 (1976) 2241-2251.
- [45] E.A. Boucher, P.M. Hines, Properties of aqueous salt solutions of poly(ethylene oxide): Thermodynamic quantities based on viscosity and other measurements, *Journal of Polymer Science: Polymer Physics Edition*, 16 (1978) 501-511.
- [46] B. Fortier-McGill, V. Toader, L. Reven, Chain Dynamics of Water-Saturated Hydrogen-Bonded Polymer Complexes and Multilayers, *Macromolecules*, 44 (2011) 2755-2765.
- [47] C.D. Magnusson, M.A. Kelland, Study on the Synergistic Properties of Quaternary Phosphonium Bromide Salts with N-Vinylcaprolactam Based Kinetic Hydrate Inhibitor Polymers, *Energy & Fuels*, 28 (2014) 6803-6810.

- [48] S.-P. Kang, E.S. Kim, J.-Y. Shin, H.-T. Kim, J.W. Kang, J.-H. Cha, K.-S. Kim, Unusual synergy effect on methane hydrate inhibition when ionic liquid meets polymer, *RSC Advances*, 3 (2013) 19920-19923.
- [49] Y.E. Kirsh, N.A. Yanul, K.K. Kalninh, Structural transformations and water associate interactions in poly-N-vinylcaprolactam–water system, *European Polymer Journal*, 35 (1999) 305-316.
- [50] L. Keshavarz, J. Javanmardi, A. Eslamimanesh, A.H. Mohammadi, Experimental measurement and thermodynamic modeling of methane hydrate dissociation conditions in the presence of aqueous solution of ionic liquid, *Fluid Phase Equilibria*, 354 (2013) 312-318.
- [51] K. Tumba, P. Reddy, P. Naidoo, D. Ramjugernath, A. Eslamimanesh, A.H. Mohammadi, D. Richon, Phase Equilibria of Methane and Carbon Dioxide Clathrate Hydrates in the Presence of Aqueous Solutions of Tributylmethylphosphonium Methylsulfate Ionic Liquid, *Journal of Chemical & Engineering Data*, 56 (2011) 3620-3629.
- [52] S. Budavari, *The merck index: An encyclopedia of chemicals, drugs and biologicals*, Merck & Co., Inc., 2274.
- [53] N. Daraboina, C. Malmos, N. von Solms, Synergistic kinetic inhibition of natural gas hydrate formation, *Fuel*, 108 (2013) 749-757.
- [54] J.D. Lee, P. Englezos, Enhancement of the performance of gas hydrate kinetic inhibitors with polyethylene oxide, *Chemical Engineering Science*, 60 (2005) 5323-5330.
- [55] W. Lee, J.-Y. Shin, K.-S. Kim, S.-P. Kang, Synergetic Effect of Ionic Liquids on the Kinetic Inhibition Performance of Poly(N-vinylcaprolactam) for Natural Gas Hydrate Formation, *Energy & Fuels*, (2016).

Table 1: List of Used Inhibitors or Synergents for CH₄ Hydrate Inhibition

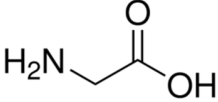
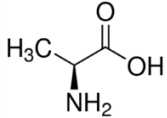
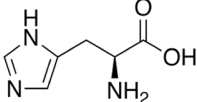
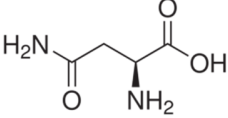
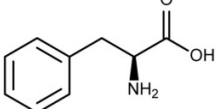
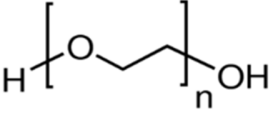
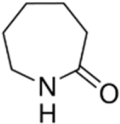
Amino Acid	Structure	M.W. (g/mol)	Purity (%)	Supplier
Glycine		75.06	≥98.5	Sigma-Aldrich
L-Alanine		89.09	≥99.5	Sigma
L-Histidine		155.15	≥99.5	Sigma
L-Asparagine		132.12	≥98.0	Sigma
L-Phenylalanine		165.19	≥99.0	Sigma
Polyethylene Oxide		≈ 100,000	≥98.0	Sigma-Aldrich
VinylCaprolactum		139.19	≥98.0	Sigma-Aldrich

Table 2: Pure CH₄ gas-hydrate equilibrium calibration experimental data and literature comparison.

Reference [50]		Reference [51]		This Work*	
T (°C)	P (bars)	T (°C)	P (bars)	T (°C)	P (bars)
1.55	30.5	4.15	38.8	4.098	38.7
1.65	30.6	10.75	77.7	5.31	42.35
3.75	37.1	11.65	86.4	7.99	57.63
5.65	45.8	11.75	86.8	8.87	61.30
7.75	55.2	14.35	116.5	10.52	75.18
8.15	57.2	15.35	131.6	12.94	98.59
8.85	62.9			14.33	119.23

*Standard uncertainties, u , are $u(P) = 0.02$ bar, $u(T) = 0.25$ °C

Table 3: CH₄ Hydrates Dissociation Points (P-T) Obtained in the Presence of the Amino Acids at Different Concentrations.

Amino Acids	P (bars)	T (°C)	Amino Acids	P (bars)	T (°C)
	116.69	14.23		110.49	12.86
	97.63	12.73		94.80	11.81
L-Alanine at 1 wt. %	76.95	10.70	L-Alanine at 5 wt. %	75.83	9.76
	57.78	8.04		56.71	7.17
	39.05	4.27		38.08	3.42
	118.96	14.40		96.06	11.91
	97.55	12.73		76.99	9.95
Glycine at 1 wt. %	77.04	10.63	Glycine at 5 wt. %	57.09	7.26
	58.16	8.01		39.20	3.48
	38.89	4.18		-	-
	118.40	14.45		113.40	13.66
	97.99	12.84		98.45	12.69
Histidine at 1 wt. %	78.21	10.91	Histidine at 4 wt. %	76.17	10.44
	60.28	8.47		58.56	8.02
	40.11	4.51		40.74	4.57
	112.33	14.00		105.09	13.48
	95.15	12.57		97.67	12.91
L-Asparagine at 1 wt. %	76.30	10.56	Phenylalanine at 1 wt. %	80.29	11.18
	57.43	7.95		60.27	8.50
	38.22	3.88		40.14	4.53

*Standard uncertainties, u , are $u(P) = 0.02$ bar, $u(T) = 0.25$ °C

Table 4: CH₄ Hydrates Formation or Induction Points (t-P) in the Presence of Amino Acids at Different Concentrations.

Amino Acids	P (bars)	t (hrs)	Amino Acids	P (bars)	t (hrs)
	115.35	5.06		109.22	5.10
	97.02	5.12		93.76	5.77
L-Alanine at 1 wt. %	76.64	6.04	L-Alanine at 5 wt. %	75.17	7.00
	57.37	7.74		56.30	8.17
	38.80	9.81		37.85	10.10
	118.06	4.10		115.14	5.11
	95.92	5.84		95.16	5.40
Glycine at 1 wt. %	76.53	5.96	Glycine at 5 wt. %	76.21	6.75
	57.79	7.70		56.03	9.33
	38.68	9.69		39.05	9.98
	117.54	4.29		111.96	4.79
	96.93	5.17		96.64	6.17
Histidine at 1 wt. %	77.55	6.06	Histidine at 4 wt. %	74.99	7.04
	60.05	6.99		57.76	8.33
	39.90	9.29		40.46	9.62
	110.42	5.53		104.25	4.65
	94.52	5.10		95.85	6.13
L-Asparagine at 1 wt. %	75.58	6.58	Phenylalanine at 1 wt. %	79.35	6.24
	56.60	8.50		59.66	7.53
	37.97	9.72		40.26	9.99

*Standard uncertainties, u , are $u(P) = 0.02$ bar, $u(T) = 0.25$ °C

Table 5: CH₄ Hydrates Dissociation Points (P-T) Obtained in the Presence of Amino Acids + 1wt% VCap / PEO

VCap + Amino Acids	P (bars)	T (°C)	PEO + Amino Acids	P (bars)	T (°C)
	39.57	3.34		58.25	7.86
Alanine at 5wt%	58.263	7.13	5wt% Alanine	76.83	10.84
	97.252	11.87		96.27	12.33
	116.12	13.354		116.47	14.23
	38.96	3.26		57.97	8.07
Glycine at 5wt%	57.18	6.90	Glycine at 5wt%	76.47	10.36
	75.90	9.56		94.75	12.20
	94.09	11.53		113.11	13.80
	114.53	13.13		-	-
	38.75	3.44		57.79	8.19
Histidine at 4wt%	58.62	7.59	Histidine at 4wt%	72.93	10.28
	76.97	10.17		95.55	12.41
	95.62	12.14		114.90	13.93
	113.19	13.56		-	-

*Standard uncertainties, u , are $u(P) = 0.02$ bar, $u(T) = 0.25$ °C

Table 6: CH₄ Hydrates formation or Induction Points (t-P) Obtained in the Presence of Amino Acids + 1wt% VCap / PEO

VCap+ Amino Acids	P (bars)	t (hrs)	PEO + Amino Acids	P (bars)	t (hrs)
	39.39	9.9639		56.20	35.10
Alanine at 5wt%	57.96	7.8167	Alanine at 5wt%	71.74	13.85
	68.39	6.979		86.06	12.39
	96.58	5.375		98.50	12.75
	38.92	9.94		56.29	30.31
Glycine at 5wt%	56.85	7.97	Glycine at 5wt%	64.84	16.26
	75.87	6.51		81.49	12.61
	94.70	5.39		100.65	11.40
	113.68	4.75		-	-
	38.50	9.90		55.12	26.94
Histidine at 5wt%	58.32	7.54	Histidine at 4wt%	62.38	18.18
	76.49	6.16		83.54	12.43
	94.96	5.17		104.57	10.61
	112.71	4.52		-	-

*Standard uncertainties, u , are $u(P) = 0.02$ bar, $u(T) = 0.25$ °C

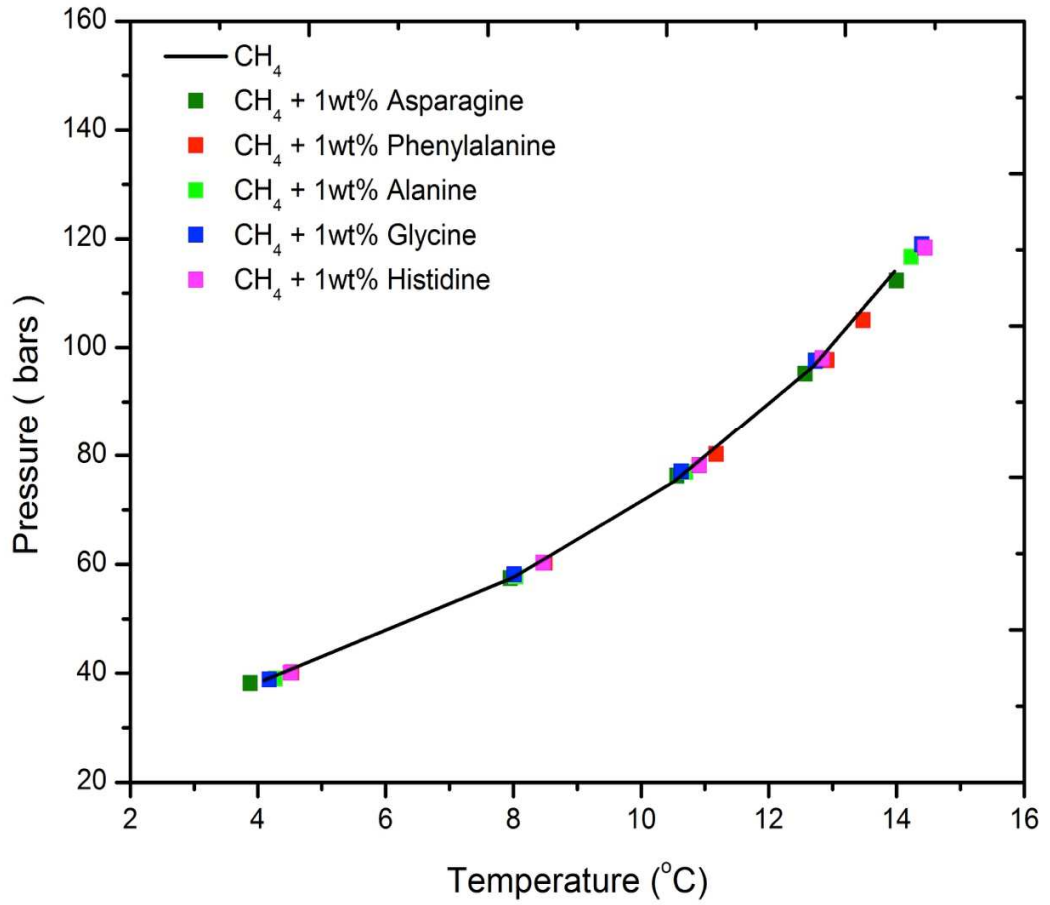


Figure 1: CH₄ hydrate dissociation points plotted against temperature and pressure for thermodynamic hydrate inhibition performance in presence of amino acids at 1 wt%.

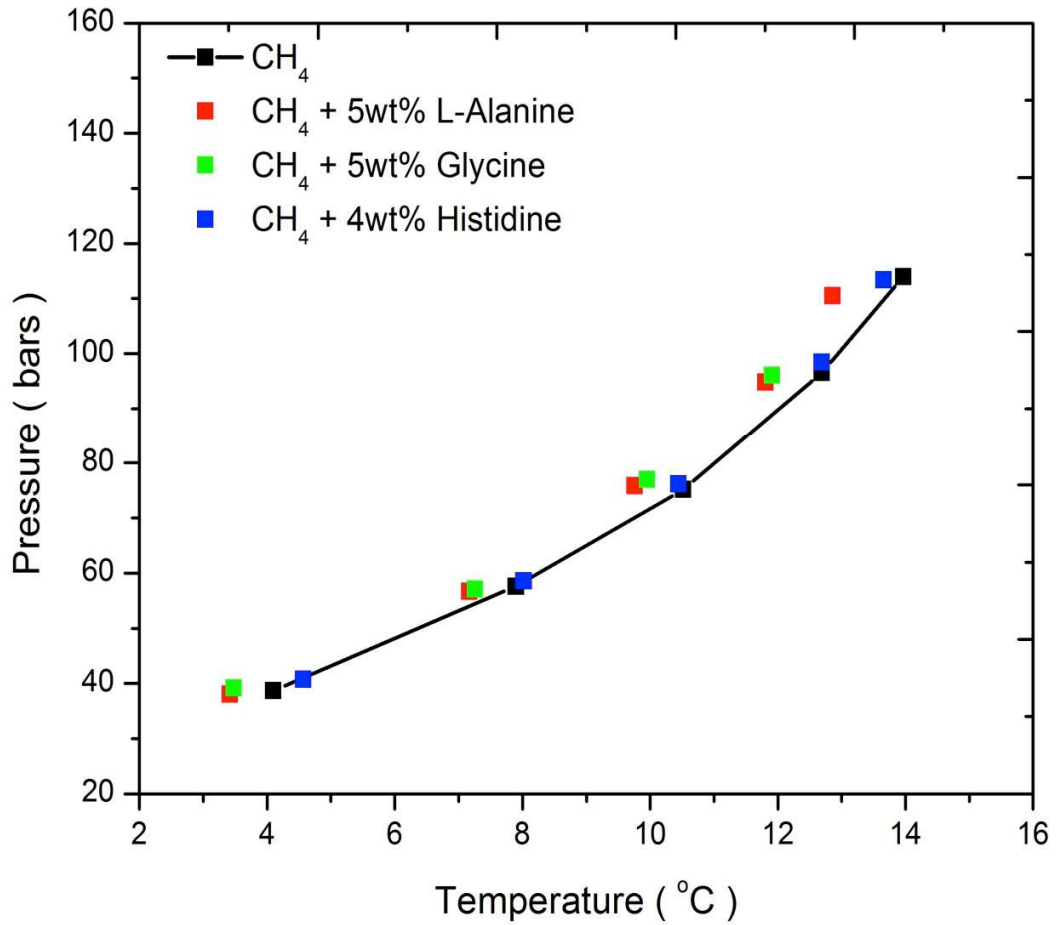


Figure 2: CH₄ hydrate dissociation points plotted against temperature and pressure for thermodynamic hydrate inhibition performance in presence of amino acids at 5 or 4 wt%.

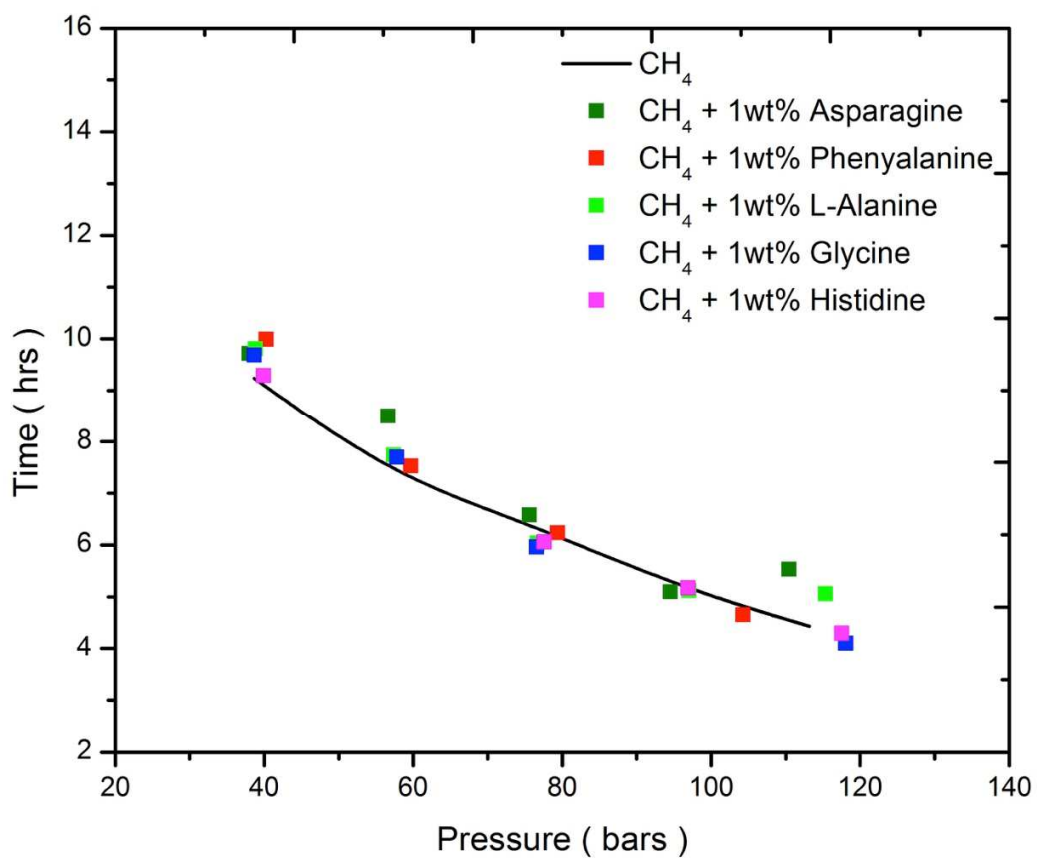


Figure 3: CH₄ hydrate induction points plotted against time and pressure for kinetic hydrate inhibition performance in presence of amino acids at 1 wt%.

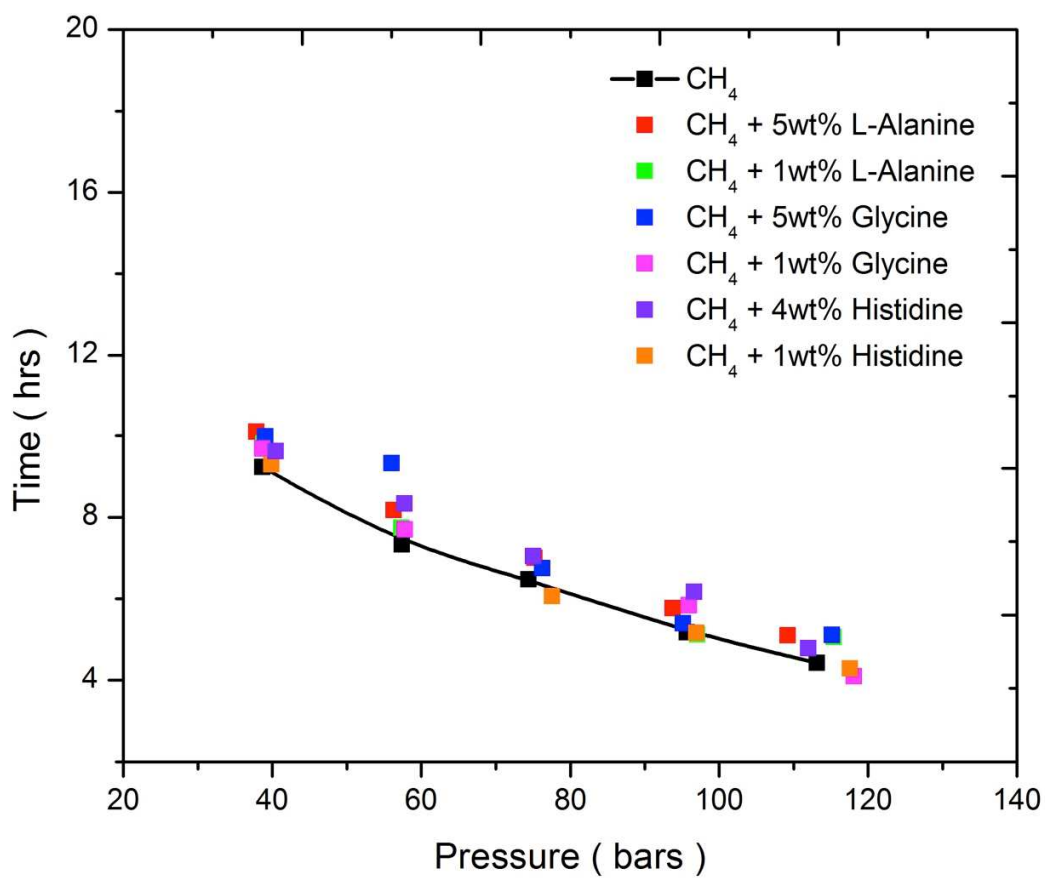


Figure 4: CH₄ hydrate induction points plotted against time and pressure for kinetic hydrate inhibition performance in presence of amino acids at 1, 4 and 5 wt%.

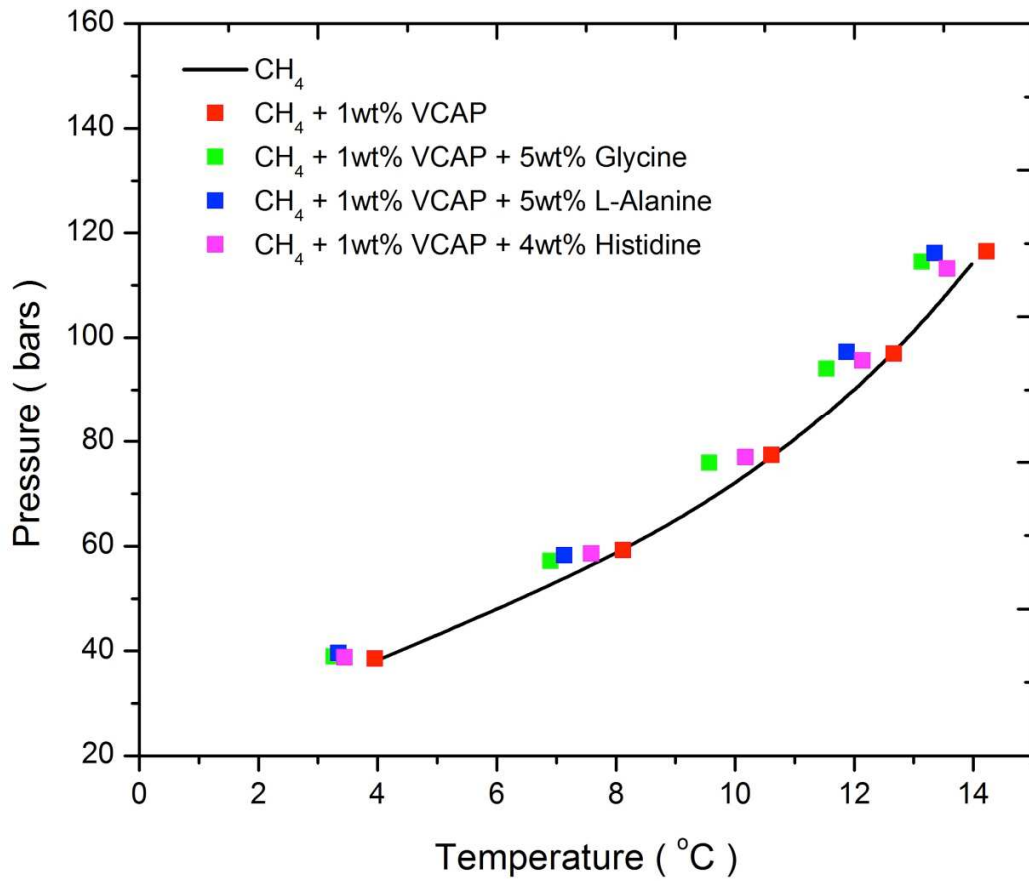


Figure 5: CH₄ hydrate dissociation points plotted against temperature and pressure for thermodynamic hydrate inhibition performance in presence of amino acids at 4 and 5 wt% + VCap at 1 wt%.

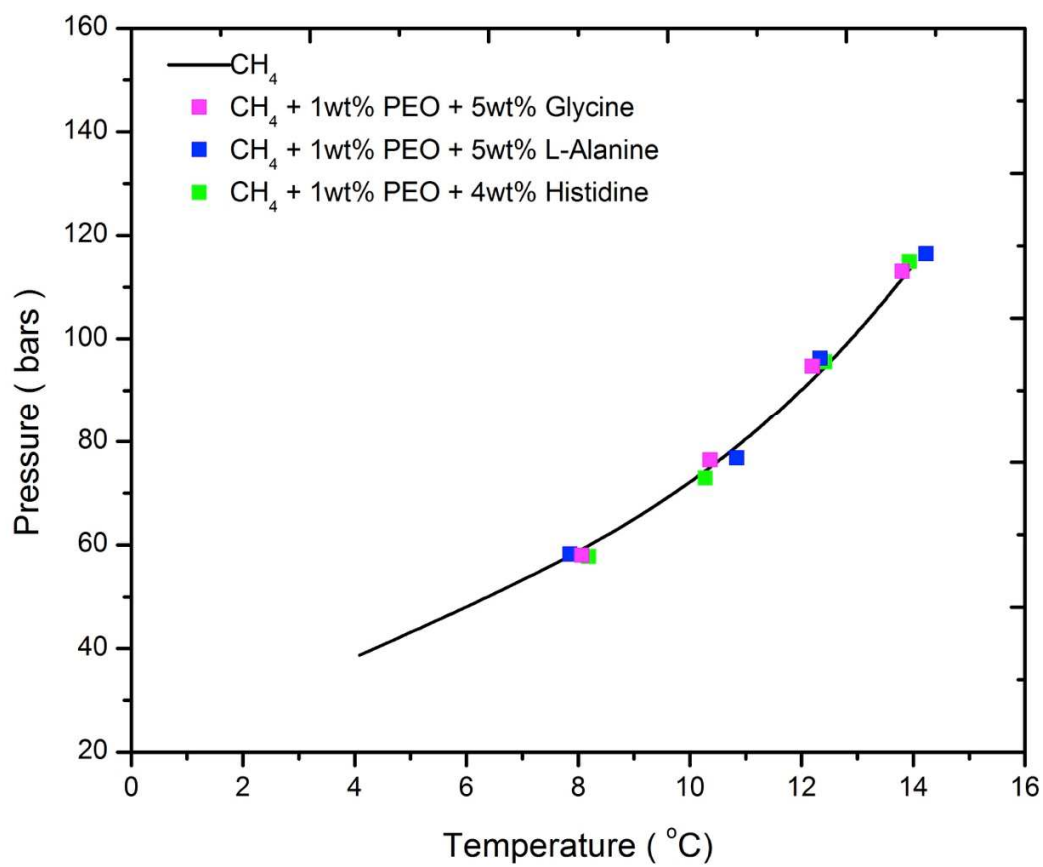


Figure 6: CH₄ hydrate dissociation points plotted against temperature and pressure for thermodynamic hydrate inhibition performance in presence of amino acids at 4 and 5 wt% + PEO at 1 wt%.

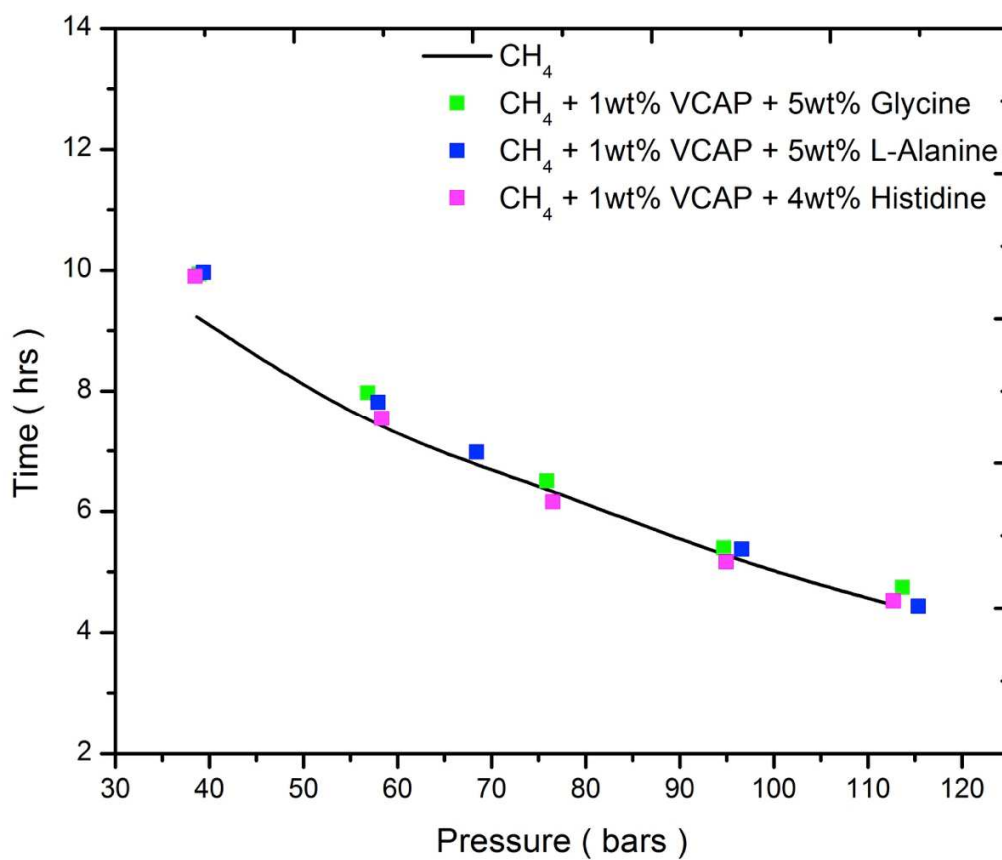


Figure 7: CH₄ hydrate induction points plotted against time and pressure for kinetic hydrate inhibition performance in presence of amino acids at 4 and 5 wt% + VCap at 1 wt%.

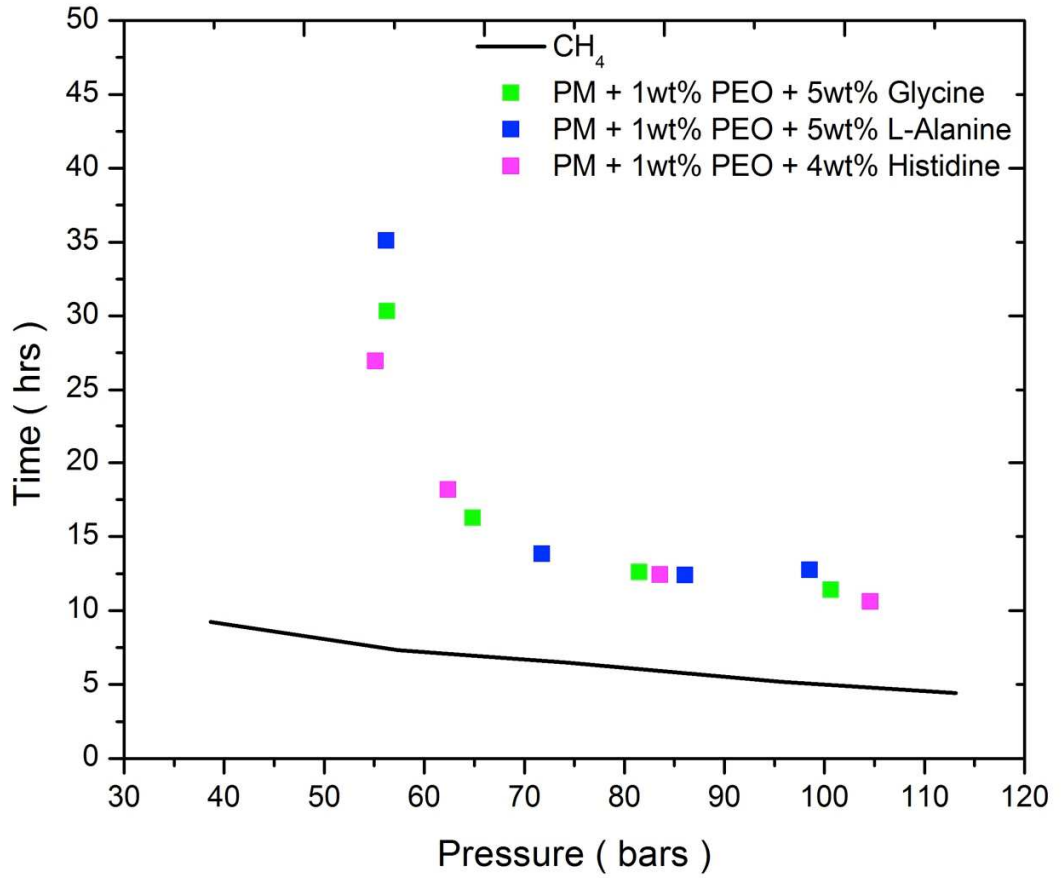


Figure 8: CH₄ hydrate induction points plotted against time and pressure for kinetic hydrate inhibition performance in presence of amino acids at 4 and 5 wt% + PEO at 1 wt%.

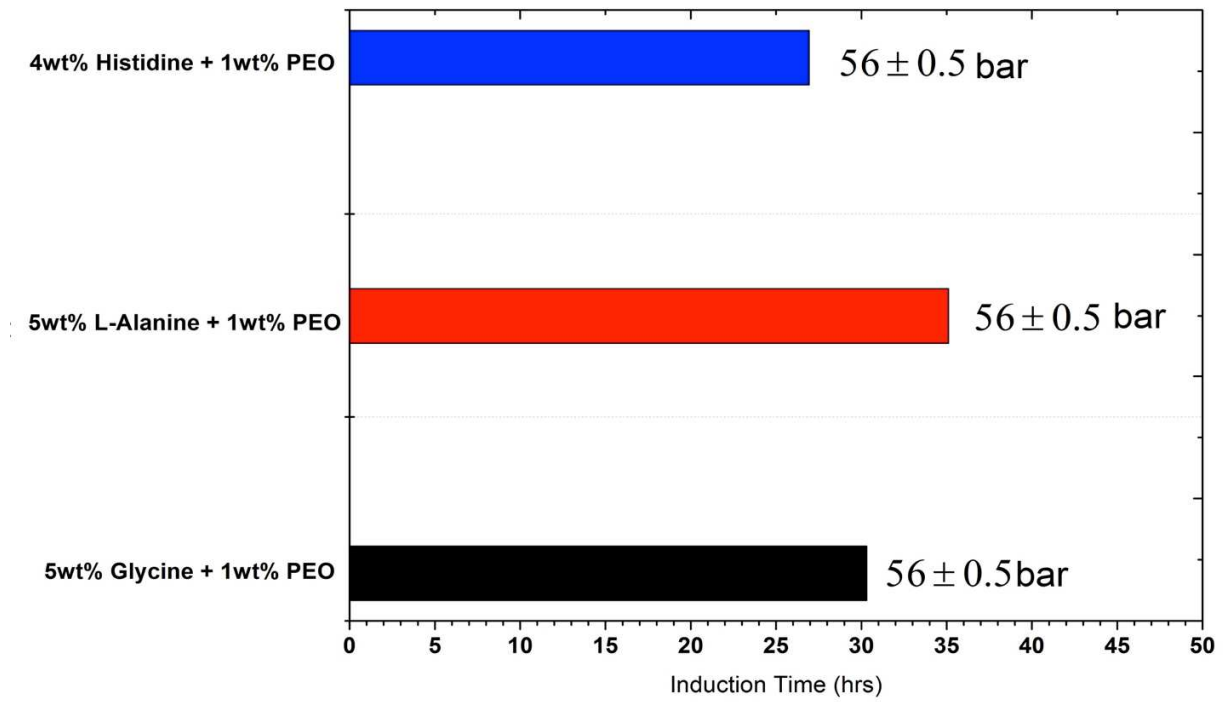


Figure 9: Comparative Induction time of amino acids for kinetic inhibition performance

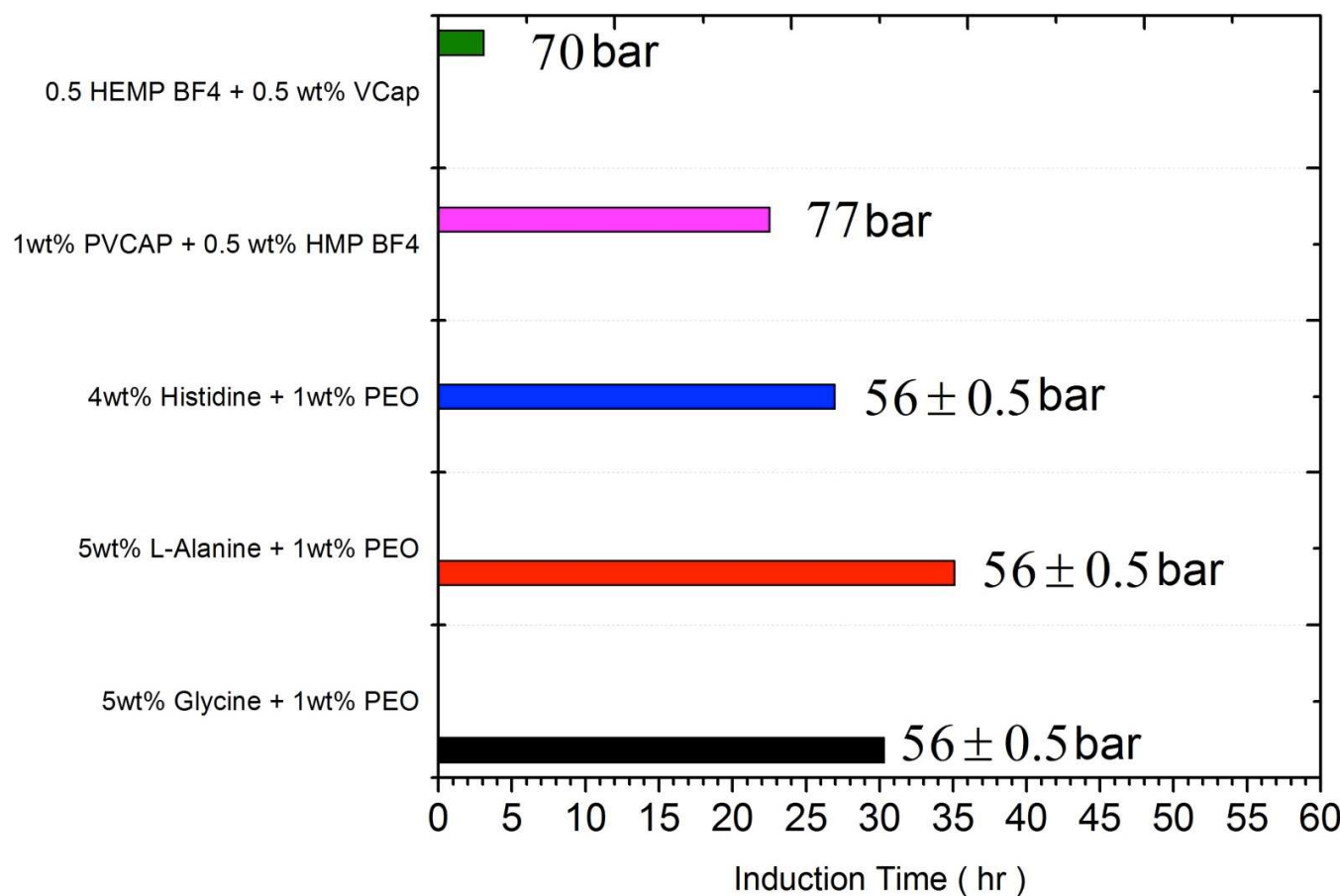
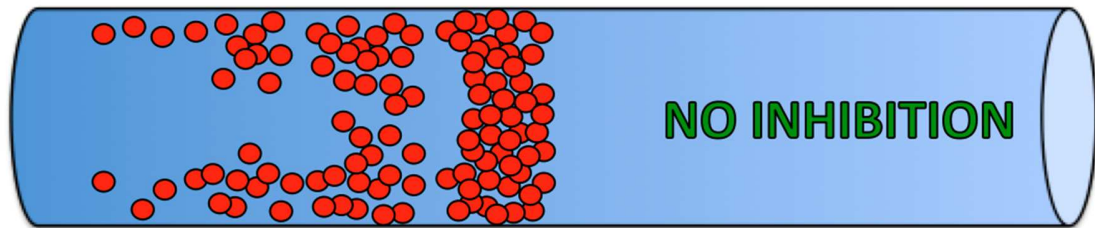


Figure 10: Comparative induction time for synergistic effect in presence of amino acids + PEO of this work and ionic liquids + PVCap at different pressures, (Green Bar - RSC Adv, 2013, 3(43), pp. 19920-19923), (Pink Bar - Energy & Fuels Energy Fuels, 2016, 30 (11), pp 9162–9169).

Graphical Table of Content



NATURAL GAS HYDRATE FORMING IN PIPELINES

